

A CNN-RNN Framework for Image Annotation from Visual Cues and Social Network Metadata

Tobia Tesan Pasquale Coscia Lamberto Ballan

Department of Mathematics “Tullio Levi-Civita”, University of Padova, Italy

{tobia.tesan}@studenti.unipd.it, {pasquale.coscia, lamberto.ballan}@unipd.it

Abstract

Images represent a commonly used form of visual communication among people. Nevertheless, image classification may be a challenging task when dealing with unclear or non-common images needing more context to be correctly annotated. Metadata accompanying images on social-media represent an ideal source of additional information for retrieving proper neighbourhoods easing image annotation task. To this end, we blend visual features extracted from neighbours and their metadata to jointly leverage context and visual cues. Our models use multiple semantic embeddings to properly map metadata to a meaningful semantic space decoupling the neural model from the low-level representation of metadata and achieve robustness to vocabulary changes between training and testing phases. Convolutional and recurrent neural networks (CNNs-RNNs) are jointly adopted to infer similarity among neighbours and query images. We perform comprehensive experiments on the NUS-WIDE dataset showing that our models outperform state-of-the-art architectures based on images and metadata, and decrease both sensory and semantic gaps to better annotate images.

1. Introduction

Images represent an effective and immediate form of expression commonly used to share events and moments of our daily lives. This is particularly true nowadays with the rising popularity of social networks such as Facebook, Twitter and Instagram. Additional information like similar images and social network *metadata*, are often employed to provide external context and to emphasize moods and messages. Dealing with such contextual data could advantage visual recognition tasks, such as image tagging and retrieval [24], in ambiguous cases where main parts are occluded or unrecognizable (as in Figure 1). In this paper we build on the intuition that a context of additional weakly-annotated images can help in disambiguating the visual classification

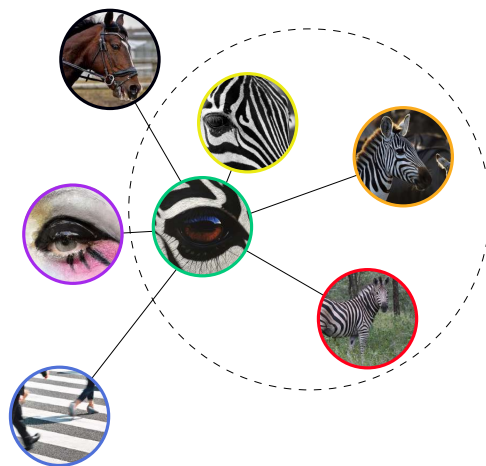


Figure 1: Some images might be hard to recognize without additional context even for humans. However, related images on a network typically share similar *metadata*. Based on this intuition, given a test image x , we retrieve a neighbourhood of images sharing similar metadata (e.g., tags) to assist the automatic image annotation task. Our approach builds on [20] and introduces more advanced semantic mapping and CNN-RNN fusion schemes.

task, as shown in the seminal work by Johnson *et al.* [20].

The idea of using contextual data to improve visual recognition is not new [35, 9]. Even humans usually benefit from the context in object detection and scene recognition [31]. In particular, in this work we exploit the (noisy) contextual information given by metadata embedded in images shared on social-networks. Metadata could be very useful to classify examples that occur very rarely or showing visual elements in non-prototypical views. Here image and social-network metadata can be considerably effective in bridging the sensory and the semantic gap [5, 28].

Various types of metadata are shared on social-networks. For example, digital photos normally provide information like ISO, exposure, location or timestamp. Users may also

add textual descriptions, or provide names of people which appear in photos. Several works have exploited metadata to improve image classification and retrieval, mostly using user-generated tags [13, 14, 18, 30, 12, 26], GPS data [15, 41, 34] or groups [38]. In [20], image metadata such as tags¹ or Flickr groups are used nonparametrically to generate a pool of related images, that can be further exploited by a deep neural network to blend visual information from a given image and its neighborhood. The key contribution of the approach is a model that can deal with different metadata and adapts over time with no (or very limited) re-training. Thus the model reported state-of-the-art results on multilabel image annotation by taking advantage of strong visual models [21, 11] and flexible nonparametric approaches [37, 40].

In this work we explore different architectures based on both visual cues and external data (e.g., tags) to improve the simple fusion scheme presented in [20]. More specifically, we first focus on preserving distance between a test image x and its neighbours to capture more relevant labels, as well as on handling vocabulary changes when new terms are included. To this end, our proposed architectures attempt to better encode the semantic meaning of tags through word embeddings [29, 33]. Second, we investigate and design different architectures for image-to-neighborhood features fusion. Here the main source of inspiration is given by recent CNN-RNN models for image classification and captioning [39, 25]. In these works, a CNN is used to extract the image feature vector, which is then fed into an RNN that either decodes it into a list of labels (multilabel image classification) or a sequence of words composing a sentence (captioning). In contrast, we investigate different strategies in which an RNN is used to sequentially blend the visual or multimodal information in a joint feature space.

The remainder of the paper is organized as follows. In Section 2, we first review related work in the area of image classification in a (noisy) multimodal scenario. In Section 3, we present our deep network framework. We evaluate the performance of our method on the NUS-WIDE dataset [4], and Section 4 shows that the approach improves previous state-of-the-art models [20, 39]. Moreover, we plan to make our trained models and code publicly available.

2. Related Work

Image tagging and retrieval. The idea of harvesting images from the web to train visual classification models has been explored many times in the past [10, 23, 7, 3, 32]. Despite its simplicity, a popular and quite effective approach for automatic image annotation, that has been often used in early works, is nearest-neighbors based label transfer [27, 37]. More recently, deep networks have been applied

extensively also in this domain achieving state-of-the-art results on many popular benchmarks [21, 11].

Among the vast literature on image tagging and retrieval [24], our work is mostly related to multimodal representation learning of images and labels. To this end, early works often model the association between visual data and labels in a generative way [1, 22, 2] or rely on mapping images and labels to a common semantic space using techniques such as CCA or KCCA [18, 36]. Finally, Hu *et al.* [17] observe that diverse levels of visual categorization are possible depending on the level of desired abstraction. Thus, they rely on structured inference to capture relationships among concepts in neural networks. In general, these approaches demonstrate the benefit of exploiting side information and multimodal correlations between visual features and labels, but they only rely on ground truth annotations.

Automatic image annotation with metadata. Several previous works tackled the automatic image annotation task using social-network metadata [5, 15, 28, 38]. User-generated tags are significantly the most commonly used metadata for multilabel image classification. In [14], Guillaumin *et al.* consider a scenario in which only visual data is used at test time, but metadata from social media websites (such as Flickr) are available at training time and can be leveraged to improve classification using semi-supervised learning. Moreover, a combination of simple nonparametric models and metric learning is used in [13], while [40] focuses on selecting a better set of training images to drive the label transfer. Flickr groups are exploited in [38] to derive a measure of image similarity which can encode broader correlations than user-generated tags and labels. A graph over tags, groups or common GPS location is used by Niu *et al.* [30] to define a semi-supervised topic model for image classification. Similarly, a CRF model over visual features, tags and GPS data is used in [8] for image clustering.

Our work falls in this area. Inspired by the model presented by Johnson *et al.* [20], we also use a deep network to blend the visual information extracted from a neighborhood of images sharing similar metadata. This idea has been also recently followed in [42] where a co-attention mechanism is used to construct a graph in which each node represents a relevant neighbour and correlated images are connected by edges. Our method differs from these works because we focus on defining a more effective architecture to combine visual cues and social-network metadata from both the test image and the neighborhood.

3. Our Framework

Our goal is to annotate images using side information carried by their neighbours. More specifically, we jointly exploit visual features as well as tags which commonly accompany images on social networks. Tags are embedded

¹Not to be confused with ground-truth *labels* we wish to predict.

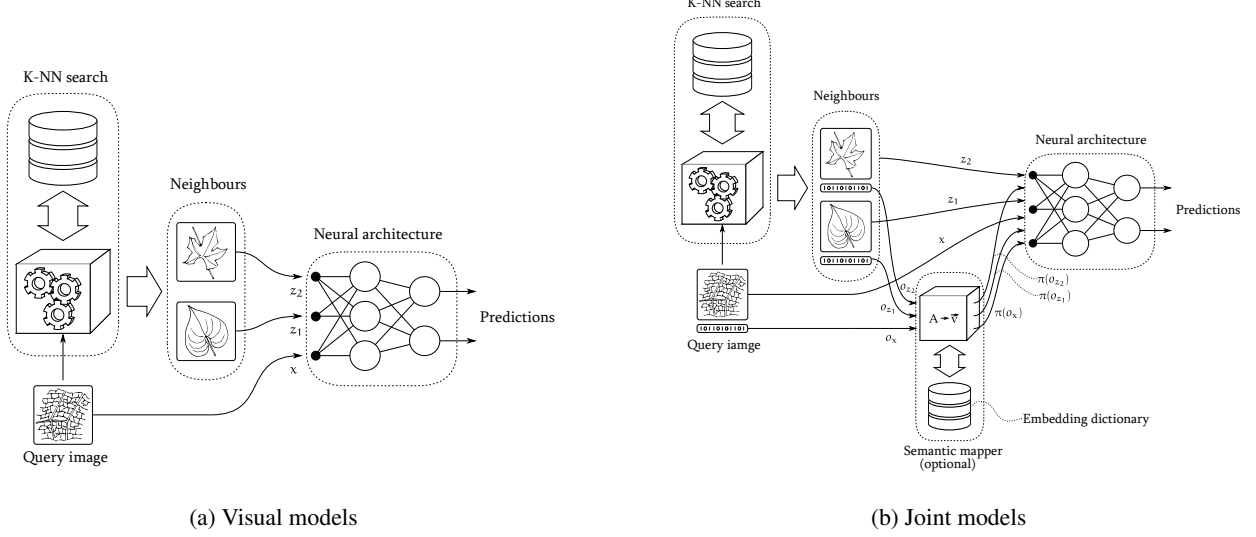


Figure 2: General architectures of the proposed models. A K-Nearest Neighbours approach is used to retrieve similar images using metadata, while a neural network processes the retrieved information. (a) shows the architecture for visual models (as proposed in [20]) where only visual features for both query image and neighbours are used to predict labels. (b) shows the architecture for joint models where metadata are also fed, possibly after a transformation step, to the final classification layer.

using different semantic mappings. Our models are built upon the work presented by Johnson *et al.* [20], where metadata are only used to retrieve similar images and the annotation task mainly relies on visual features.

We propose two general architectures for images annotation, both based on visual features and image metadata (see Figure 2). Based on such architectures, we define two set of models, namely visual and joint models. Whereas visual models only exploit visual cues, joint models handle metadata which are directly fed to the neural network after a transformation step.

All the models generate nonparametrically a neighbourhood Z_x for a query image x using metadata and then the networks are trained to classify x given its neighbours in Z_x . The neighbourhood generation process is parametrized over a neighbourhood size m and a max rank M . More specifically, let Z_x be the M -nearest neighbours of x according to a distance measure δ . The set of candidate neighbourhoods for an image x is the set:

$$Z_x = \{s \in \mathcal{P}(X) : |s| = m\}, \quad (1)$$

where $\mathcal{P}(X)$ denotes the power set of X , that is the set of considered images. The prediction $s(x, \theta)$ is the average of $f(x, \vec{z}; \theta)$ over all candidate neighbourhoods:

$$s(x, \theta) = \frac{1}{|Z_x|} \sum_{z \in Z_x} f(x, \vec{z}; \theta), \quad (2)$$

where x is the image to be classified, $\vec{z} = (z_1, z_2, \dots, z_m)$

are the neighbours and $f(x, \vec{z}; \theta)$ is the output of the neural network which takes into account their visual cues.

The model is trained by computing a loss function \mathcal{L} and minimizing:

$$\theta^* = \arg \min_{\theta} \sum_{(x, y) \in D_{train}} \mathcal{L}(s(x, \theta), y), \quad (3)$$

where y represent a subset of all possible labels that appear in D . Note that neighbours are ordered according to their distance when fed to the neural network.

A variation is considered in the case of joint models, in which metadata are directly fed to the final layer of the network, eventually after a transformation step $\pi(\cdot)$ which involves a lookup in a dictionary of semantic embeddings. In this case, the prediction $s(x, \theta)$ is the average of $f(x, \pi(o_x), \vec{z}, \pi(\vec{o}_z); \theta)$, where o_x is the metadata vector for image x while $\pi(o_x)$ is its transform. We shall use $\pi(\vec{o}_z)$ as shorthand for $\text{map}(\pi, \vec{o}_z) = (\pi(o_{z_1}), \pi(o_{z_2}), \dots, \pi(o_{z_m}))$, where \vec{o}_z are metadata vectors for the neighbourhood.

3.1. Metadata Encoding

Metadata representation may affect networks ability to recover correct annotations. For this reason, we firstly encode metadata without associating any meaningful representation to each word, i.e., semantically close words could be associated to distant vectors, and secondly consider more powerful word encoding techniques.

One-hot encoding. We focus on social-network tags represented as binary vectors $o_x \in \{0, 1\}^\tau$. More specifically, let x the query image and $(t_{(1)}, t_{(2)}, \dots, t_{(n)})$ all relevant tags for x chosen from a vocabulary of τ tags, the binary vector o_x is the sum of the one-hot vectors for each of its tags:

$$o_x = \sum_{i \text{ s.t. } t_i \in \{t_{(1)}, t_{(2)}, \dots, t_{(n)}\}} e_i^\tau. \quad (4)$$

Using `id`, i.e., raw binary vectors, neighbourhoods are computed using the Jaccard distance \mathcal{J} between binary vectors as distance measure. Binary vectors o_x for each image x (or neighbour z_i) are directly handled by the neural network, without further processing. The Jaccard distance² is defined as:

$$\mathcal{J}(x, x') = 1 - \frac{|t_x \cap t_{x'}|}{|t_x \cup t_{x'}|} \quad (5)$$

with $\mathcal{J}(x, x) = 0$.

Semantic-aware encoding. We also explore more powerful word embedding techniques in order to encode similar word into similar vectors. We consider a transformation that maps a vector o_x to a *semantic space* $\pi : \{0, 1\}^\tau \rightarrow \mathbb{R}^n$. It is clear that, unlike visual models, where metadata are used implicitly, a neural network trained to make predictions as a function of one or more binary vectors becomes useless if the vocabulary changes. Semantic maps π can decouple the low-level bit representation from the semantic meaning, making models learned on a tag vocabulary applicable to a different one, as long as an appropriate $\tilde{\pi}$ is available that maps the *new* binary vectors onto the *old* semantic space. More specifically, given a map or dictionary of embeddings $\beta : TAGS \rightarrow \mathbb{R}^n$ for some n , we define $\rho(o_x; \beta)$ as the sum of the vectors $\beta(t_{(i)})$ for each tag $t_{(i)}$ relevant for image x , i.e.:

$$\rho(o_x; \beta) = \sum_{i=1}^{\tau} o_{x(i)} \cdot \beta(t_{(i)}). \quad (6)$$

For $\pi(x) = \rho(o_x; \beta)$, we consider two semantic embeddings. Firstly, we use a dictionary of `word2vec` embeddings [29]; they are obtained by training on a 100-billion-words subset of the Google News database and contain 300-dimensional vectors for 3 million words and phrases. We expect to recover some semantic information from the tags and improve performance, as well as achieving decoupling from the low-level binary representation for joint architectures. We choose cosine distance for δ , defined as:

$$\text{sim}_{\cos}(x_1, x_2) = 1 - \frac{\vec{x}_1 \cdot \vec{x}_2}{|\vec{x}_1| |\vec{x}_2|}. \quad (7)$$

²The complement of Jaccard similarity, i.e. intersection-over-union.

Secondly, we use `WordNet` embeddings which works in the same fashion as `word2vec` embeddings, except that β is extracted from a dictionary where vector representations are optimized to be similar if the words are close on the WordNet ontological graph. Cosine distance is again the choice of δ . WordNet embeddings [33] comprise a dictionary of 650-dimensional vectors obtained from Princeton WordNet 3.0³ with 60,000 words.

3.2. Visual Models

Visual models only rely on extracted visual features of input images without considering additional information. We consider three visual models based on fully-connected and recurrent layers.

Visual-only. This architecture acts as baseline; it simply amounts to a fully-connected layer over visual features $\phi(x)$ output by a CNN for an image x . Therefore,

$$f(x, \vec{z}; \theta) = W_y \Phi(x) + b_y \quad (8)$$

Note that \vec{z} is not used.

LTN. This is the model proposed in [20]. The label scores are computed as follows:

$$f(x, \vec{z}; \theta) = W_y \begin{bmatrix} v_x \\ v_z \end{bmatrix} + b_y \quad (9)$$

where $\vec{z} = (z_1, z_2, \dots, z_m)$ is a vector of neighbours obtained nonparametrically, x is the image to be classified, and

$$v_x = \sigma(W_x \Phi(x) + b_x), \quad (10)$$

$$v_z = \max_{i=1, \dots, m} (\sigma(W_z \Phi(z_i) + b_z)) \quad (11)$$

where σ is a ReLU activation function. The model is depicted in Figure 3a. Note that the weights W_z and b_z are shared among all (z_1, z_2, \dots, z_m) and $v_x, v_z \in \mathbb{R}^h$.

RTN. This architecture extends LTN by replacing the max-pooling operation with a RNN in order to better discriminate individual neighbours. More specifically, the hidden state v_z is defined as follows:

$$v_z = RNN((z_1, z_2, \dots, z_m); W_{RNN}), \quad (12)$$

where the notation $RNN((i_1, \dots, i_n), W)$ denotes a recurrent neural network sequentially fed with inputs (i_1, \dots, i_n) while W are the corresponding parameters. In this case, RNN is a long short-term memory (LSTM) network with linear activation function. The other parameters remain unchanged. The model is depicted in Figure 3b.

³<https://github.com/nlx-group/WordNetEmbeddings>

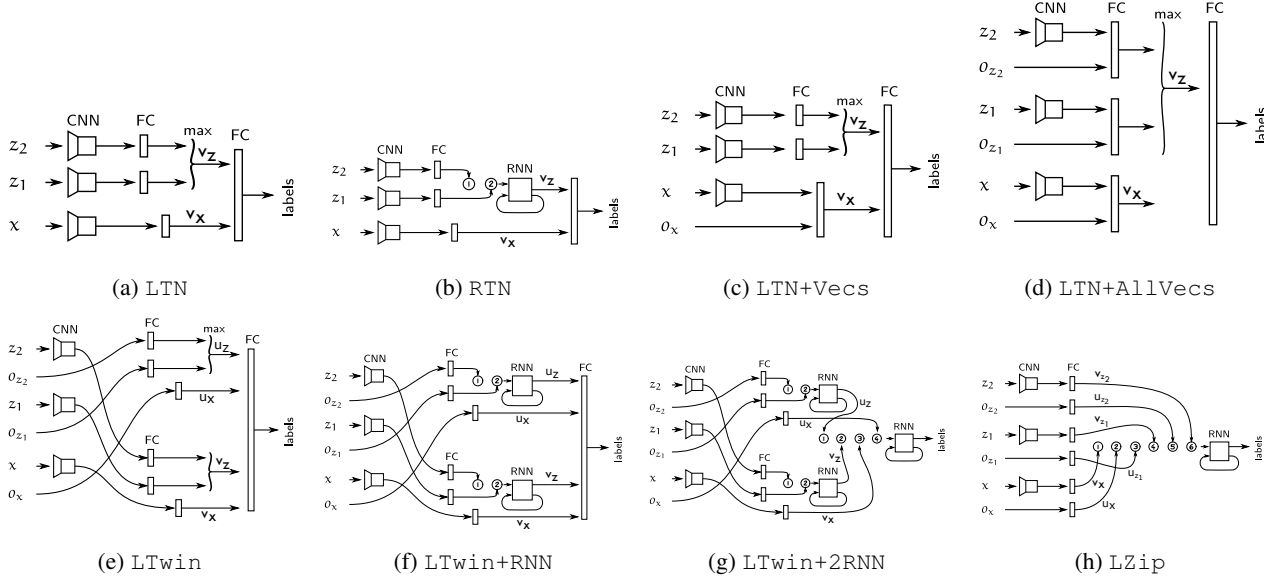


Figure 3: Our architectures which leverage image features along with their metadata. (a), (b) represent two visual models where metadata are not employed. (c) – (h) are different ways to fuse image features and metadata. In this work, as metadata we only use tags and we exploit recurrent layers and semantic embeddings in order to leverage contextual information.

3.3. Joint Models

Joint models are directly fed with metadata instead of leveraging metadata only implicitly along with visual features. Metadata improve the semantic level detected by extracted visual features. In the following, we define several architectures handling metadata (or their embeddings) using linear and recurrent layers.

LTN+Vecs. This architecture makes use of metadata o_x , i.e., metadata of image to be classified, which are concatenated to the output of the CNN of image x .

The output of the network is defined as follows:

$$f(x, \pi(o_x), \vec{z}; \theta) = W_y \begin{bmatrix} v_x \\ v_z \end{bmatrix} + b_y, \quad (13)$$

where

$$v_x = \sigma \left(W_x \begin{bmatrix} \Phi(x) \\ \pi(o_x) \end{bmatrix} + b_x \right). \quad (14)$$

v_z is defined as in LTN visual model. Note that neighbour metadata vectors are not used and the model requires a transformation step to map metadata onto a new space. The model is depicted in Figure 3c.

LTN+AllVecs. This architecture, unlike the previous one, uses metadata vectors o_x of the image to be classified and metadata of its neighbours \vec{o}_z .

The output is defined as follows:

$$f(x, \pi(o_x), \vec{z}, \pi(\vec{o}_z); \theta) = W_y \begin{bmatrix} v_x \\ v_z \end{bmatrix} + b_y, \quad (15)$$

where v_x is defined as above and

$$v_z = \max_{i=1, \dots, m} \sigma \left(W_z \begin{bmatrix} \Phi(z_i) \\ \pi(o_{z_i}) \end{bmatrix} \right). \quad (16)$$

In this case, σ is a ReLU activation function. The model is depicted in Figure 3d.

LTwin. Unlike LTN+AllVecs, such architecture processes features and metadata using two separate pipelines, i.e., metadata are not concatenated with the images features. The neighbours are blended with a max-pooling layer, so the model is not able to discriminate between nearest and farthest neighbours.

The output of the network is defined as follows:

$$f(x, \pi(o_x), \vec{z}, \pi(\vec{o}_z); \theta) = W_y \begin{bmatrix} v_x \\ v_z \\ u_x \\ u_z \end{bmatrix} + b_y, \quad (17)$$

where v_x and v_z are defined as in the LTN model, while $u_x = \sigma(W_{x_u} \pi(o_x) + b_{x_u})$ and $u_z = \max_{i=1, \dots, m} \sigma(W_{z_u} \pi(o_{z_i}) + b_{z_u})$. Max-pooling is applied on both neighbours' features and their metadata. The model is depicted in Figure 3e.

LTwin+RNN. Unlike the previous architecture, such model replaces max-pooling layers with RNN networks to handle the neighbours. Once again, RNN is an LSTM with linear activation. The output is equal to LTwin architecture with $v_z = RNN((FC_{z_1}, \dots, FC_{z_m}); W_{RNN})$ and $u_z = RNN((FC_{o_{z_1}}, \dots, FC_{o_{z_m}}); W_{ORNN})$, where $FC_{(\cdot)}$ are outputs of fully-connected layers applied to image features and metadata, respectively. The model is depicted in Figure 3f.

LTwin+2RNN. This architecture differs from the previous one in that the final fully connected layer is also replaced with a RNN. The output is defined as follows:

$$f(x, \pi(o_x), \vec{z}, \pi(\vec{o}_z); \theta) = RNN((v_x, v_z, u_x, u_z); W_{f_{RNN}}), \quad (18)$$

where v_x, v_z, u_x and u_z are defined as in LTwin+RNN. The model is depicted in Figure 3g.

LZip. Finally, this architecture uses just one RNN to combine features and metadata which are separately processed by FC layers. The output is defined as follows:

$$f(x, \pi(o_x), \vec{z}, \pi(\vec{o}_z); \theta) = RNN((v_x, u_x, v_{z_1}, u_{z_1}, \dots, v_{z_m}, u_{z_m}); W_{RNN}). \quad (19)$$

The model is depicted in Figure 3h.

3.4. Implementation details

We use RMSProp algorithm with He-Zhang initialization [16] and apply dropout with $p = 0.5$. We also set batch size dimension to 64 (in lieu of 50, as found in [20]) and $h = 500$. We apply L_2 regularization with $\lambda = 3 \times 10^{-4}$ and use a learning rate of 1×10^{-4} . λ was chosen with grid search. We use early stopping with a maximum of 10 and a minimum of 3 epochs, incremented to 15 and 5 for joint models, respectively. We run experiments with (3, 6), (6, 12) and (12, 24) as choices of (m, M) . Our CNN is the implementation of AlexNet found in Caffe [21, 19], that comes with pre-trained weights for ImageNet [6], same as [20]. We only train the last layer of the CNN.

4. Experiments

Dataset. We use the NUS-WIDE dataset [4] which comprises 269,648 images uploaded on the photo sharing website Flickr, annotated with 81 ground truth labels for evaluation. NUS-WIDE is highly unbalanced over classes, whereas the tag `sky` is relevant for around 53,000 images, many classes have less than a thousand (or a hundred) images. We restrict ourselves to the fixed subset of 190,253 images used in [20, 42] for ease of comparison. The dataset comprises 422,364 unique Flickr tags, which we narrow

down to the $\tau = 5000$ most frequent tags. The dataset is randomly partitioned to form training, validation and test sets of 110,000, 40,000 and 40,253 images, respectively. We generate 5 of such splits and run all experiments on all splits (averaging the results).

Metrics. As metrics, we report per-label and per-image mean Average Precision (mAP), as well as precision and recall. Note that, in this area, the most common evaluation protocol assumes that an algorithm should assign a fixed number k of labels to each image. To this end, following prior work [11, 20, 39], we report results for $k = 3$. Since on NUS-WIDE the average number of labels per image is approx. 2.4, by assigning exactly 3 labels, no classifier can achieve unit precision and recall (thus we report on Table 1 the real upper bound for each metric). However, as also highlighted in [13, 20, 24], mAP directly measures ranking quality, so it naturally handles multiple labels and does not require to set a fixed number k . Therefore, mAP is the primary evaluation metric used further on in our evaluation.

4.1. Experimental Results

Table 1 shows our best results in comparison to several baselines and state-of-the-art models. First of all, the LTwin model outperforms the other methods on both mAP metrics. It is also important to note that for the corresponding models proposed in [20], our implementation of LTN achieves comparable results while LTN+Vecs has worse performance. Therefore, the LTwin model achieves best results showing a 10 and 2 percentage performance increase on both mAP metrics w.r.t. the corresponding LTN+Vecs baseline.

More detailed results about all the different architectures presented in Section 3 are reported in Table 2 and Table 3 (all the results refer to a neighbourhood size of $(12, 24)^4$), highlighting a vast range of different combinations of architectures and encodings. We choose to focus our attention on mAP_{lab} and mAP_{img} since they better summarize classification performances. In general, we note that mAP_{lab} is the metric that is affected the most, whereas mAP_{img} remains more stationary.

Visual Models. As shown in Figure 4, for the same neighbourhood, RTN leads to an improvement of mAP_{lab} of around 0.7 to 1.2 percentage points over LTN, in exchange for a drop of 0.2 to 0.4 percentage points of mAP_{img} . More interestingly, the gap between $\pi = \text{id}$ and word2vec is larger for RTN at low values of m . Notice how RTN with `word2vec` embeddings and a (3, 6) neighbourhood outperforms vanilla LTN with (6, 12) neighbourhood in terms of mAP_{lab} , with negligible impact on mAP_{img} . The performance of RTN begins to decline faster than LTN with $\pi =$

⁴In the supplementary material we report full results also for other combinations of the neighbourhood parameters.

Method	mAP _{lab}	mAP _{img}	rec _{lab}	prec _{lab}	rec _{img}	prec _{img}
Tag-only Model + linear SVM [28]	46.67	-	-	-	-	-
Graphical Model (all metadata) [28]	49.00	-	-	-	-	-
CNN + WARP [11]	-	-	35.60	31.65	60.49	48.59
CNN-RNN [39]	-	-	30.40	40.50	61.70	49.90
SR-RNN [25]	-	-	50.17 *	55.65 *	71.35 *	70.57 *
SR-RNN + Vecs [25] †	-	-	58.52 *	63.51 *	77.33 *	76.21 *
SRN [43]	60.00	80.60	41.50 *	70.40 *	58.70 *	81.10 *
MangoNet [42]	62.80	80.80	41.00 *	73.90 *	59.90 *	80.60 *
LTN [20]	52.78 ±0.34	80.34 ±0.07	43.61 ±0.47	46.98 ±1.01	74.72 ±0.16	53.69 ±0.13
LTN + Vecs [20] †	61.88 ±0.36	80.27 ±0.08	57.30 ±0.44	54.74 ±0.63	75.10 ±0.20	53.46 ±0.09
Upper bound	100.00 ±0.00	100.00 ±0.00	65.82 ±0.35	60.68 ±1.32	92.09 ±0.10	66.83 ±0.12
Our baseline: v-only	45.05 ±0.11	76.88 ±0.11	42.31 ±0.59	43.74 ±1.07	71.41 ±0.13	51.36 ±0.13
Our baseline: LTN _{n:id}	53.17 ±0.12	79.82 ±0.16	45.67 ±1.75	47.64 ±2.18	74.29 ±0.13	53.34 ±0.17
Our baseline: LTN + Vecs _{n:id, f:id} †	54.86 ±0.20	81.34 ±0.15	46.56 ±1.39	50.10 ±1.70	75.67 ±0.17	54.37 ±0.14
Our model: RTN _{n:w2v}	55.36 ±0.34	79.77 ±0.27	48.73 ±2.77	51.21 ±2.61	74.35 ±0.29	53.28 ±0.24
Our model: LTwin _{n:w2v, f:w2v} †	63.13 ±0.31	83.77 ±0.06	54.40 ±1.33	51.86 ±1.58	78.06 ±0.05	55.78 ±0.13

Table 1: Results on NUS-WIDE obtained with our best models and compared to other state-of-the-art methods. We run 5 splits as in [20] and report mean and standard deviation. Models that also use metadata are marked with superscript †. In our models *n* refers to the encoding used to build the neighbourhood, while *f* to the encoding used to represent image metadata. Note: models such as [25] can decide their own prediction length and are not limited by the fixed parameter *k*. In these cases (marked with superscript *) the upper bound does not apply and results are not directly comparable with other approaches.

Arch	n	mAP _{lab}	mAP _{img}
LTN	id	53.17 ±0.12	79.82 ±0.16
LTN	w2v	54.54 ±0.13	80.32 ±0.16
LTN	wnet	53.07 ±0.17	79.95 ±0.24
RTN	id	53.97 ±0.27	79.23 ±0.27
RTN	w2v	55.36 ±0.34	79.77 ±0.27
RTN	wnet	53.76 ±0.33	79.45 ±0.30

Table 2: Visual Models results for neighbourhood size $(m, M) = (12, 24)$. Column *n* refers to the metadata encoding used to build the neighbourhood.

WordNet. This leads to hypothesize that RTN is particularly sensitive to the quality of neighbourhoods it is trained on. All models improve monotonically with *m*.

Joint Models. We firstly analyze the *naive* case, i.e., $\pi = \text{id}$ (Figure 5) and then introduce semantic mapping (Figure 6). The simplest and worst-performing model is LTN+Vecs fed with raw binary vectors; it shows quasi-linear improvement w.r.t. neighbourhood. LZIP, which uses a RNN, improves uniformly upon it and achieves very good mAP_{lab} and mAP_{img} from the start but tends to exhibit a mild decrease in performance with neighbourhood size, along with LTwin+2RNN. In turn, LTwin achieves good mAP_{img} but comparatively poor mAP_{lab}; LTwin+RNN achieves roughly comparable performance, but shows linear improvement with *m*. LZIP, at small

Arch	n	f	mAP _{lab}	mAP _{img}
LTN+Vecs	id	id	54.86 ±0.20	81.34 ±0.15
LTN+AllVecs	id	id	56.61 ±0.12	81.28 ±0.21
LZip	id	id	60.64 ±0.14	82.42 ±0.32
LZip	w2v	id	61.24 ±0.51	82.36 ±0.41
LZip	w2v	w2v	60.19 ±0.57	82.32 ±0.15
LZip	id	w2v	62.33 ±0.16	82.91 ±0.18
LTwin	id	id	56.79 ±0.24	82.64 ±0.08
LTwin	id	w2v	63.09 ±0.16	83.70 ±0.14
LTwin	w2v	id	57.73 ±0.17	83.00 ±0.06
LTwin	w2v	w2v	63.13 ±0.31	83.77 ±0.06
LTwin	id	wnet	55.12 ±0.25	81.48 ±0.10
LTwin	wnet	id	56.83 ±0.24	82.64 ±0.10
LTwin	wnet	wnet	54.01 ±0.14	81.06 ±0.10
LTwin+RNN	id	id	58.87 ±0.43	82.95 ±0.08
LTwin+2RNN	id	id	62.00 ±1.44	80.52 ±2.79
LTwin+2RNN	id	w2v	63.04 ±0.22	83.02 ±0.34
LTwin+2RNN	w2v	w2v	62.33 ±0.33	82.72 ±0.37
LTwin+2RNN	id	wnet	62.35 ±0.56	82.56 ±0.26

Table 3: Joint Models results for neighbourhood size $(m, M) = (12, 24)$, and several combinations of semantic embeddings. Column *n* refers to the metadata encoding used to build the neighbourhood, while *f* to the encoding used as representation. w2v = word2vec, wnet = wordnet, while id refers to raw binary vectors.

(m, M) , and LTwin+2RNN are the best-performing models, with LTwin comfortably in the middle for mAP_{img}. Unfortunately, LZIP and LTwin+2RNN are also by far the

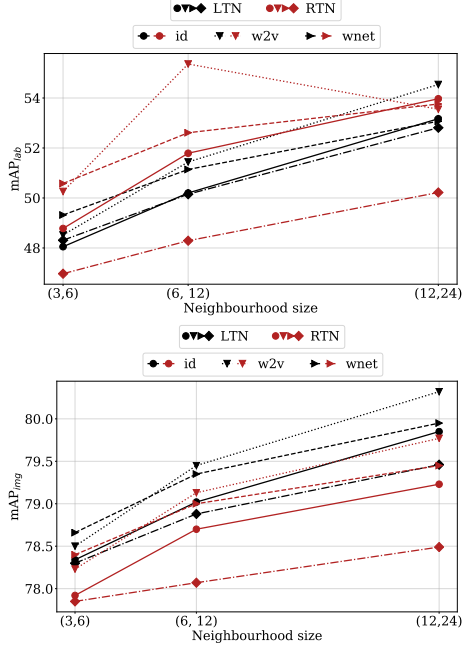


Figure 4: mAP_{lab} and mAP_{img} for visual models varying the neighbourhood size and semantic mapping to retrieve the neighbours. Black color refers to LTN model while the red one to RTN model. All the models increase their accuracy with higher values of (m, M) except RTN based on w2v semantic embedding. All the models outperform the visual-only architecture.

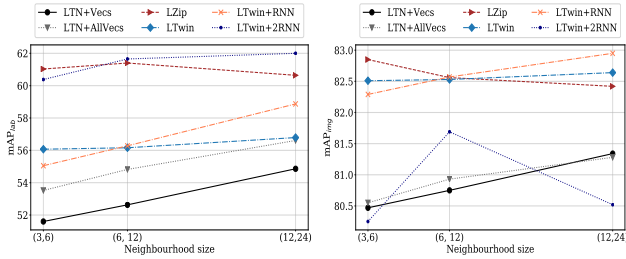


Figure 5: mAP_{lab} and mAP_{img} for joint models varying the neighbourhood size considering $\pi = id$ both for neighbours retrieval and metadata embedding.

longest to train by an order of magnitude (we just need to consider the breadth of the unrolled graph for non-trivial neighbourhood sizes).

The addition of semantic metadata transforms can give a significant boost to performance, in addition to the benefits w.r.t. robustness of the model to vocabulary changes and applicability to a different database than the one used for training. The performance of all architectures is boosted when they are fed transformations computed from word2vec vectors through Eq. 6 instead of plain binary vectors.

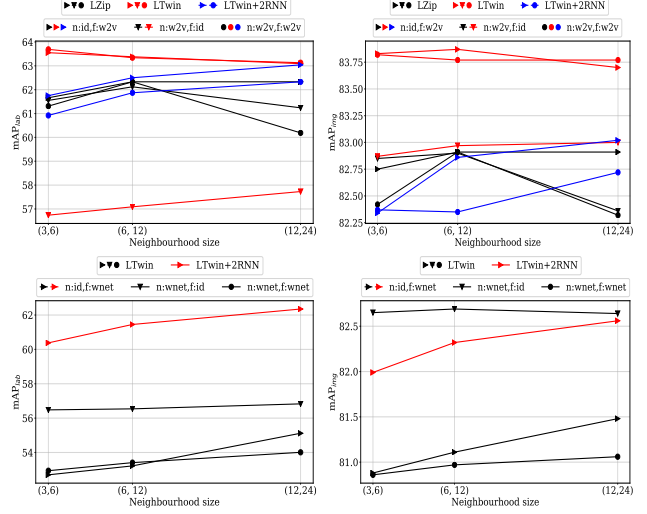


Figure 6: mAP_{lab} and mAP_{img} for joint models varying the neighbourhood size and considering $\pi = w2v$ (1st row) and $\pi = wnet$ (2nd row). Only relevant models and embedding combinations are reported. n refers to the embedding used for neighbours retrieval while f to embedding used to metadata representation.

All models tend to saturate around $(mAP_{lab}, mAP_{img}) = (.63, .83)$. This appears to be the case for LZip, even without any sort of π . It may be the case that the simpler LTwin can match the performance of the more complex models once provided with word2vec mappings. LTwin (f: word2vec) performs as well as LTwin (n: word2vec, f: word2vec), or even better; the same goes for its LZip siblings (by a considerably minor margin). We speculate that the ability of the network to learn to take maximal advantage of semantic embeddings overshadows the effect of their use in neighbourhood generation and using word2vec vectors in the neighbourhood generation process might therefore be unnecessary. LTwin (f: word2vec) emerges as the superior model. As expected, WordNet results in poor performance. Notice also how LTwin (feed: WordNet) is particularly sensitive to neighbourhood size.

5. Conclusion

We have shown that common visual models to classify images, based on metadata to retrieve neighbours, can be improved considering semantic mappings and recurrent neural networks. We have characterized the performance of a variety of visual and joint models and their variability. Our models outperform for several metrics state-of-the-art approaches. We have also shown that semantic mappings can be highly effective in improving performance, besides achieving robustness to changes in metadata vocabulary and quality of neighborhoods.

References

- [1] K. Barnard, P. Duygulu, D. Forsyth, N. De Freitas, D. M. Blei, and M. I. Jordan. Matching words and pictures. *Journal of Machine Learning Research*, 3:1107–1135, 2003.
- [2] G. Carneiro, A. B. Chan, P. J. Moreno, and N. Vasconcelos. Supervised learning of semantic classes for image annotation and retrieval. *IEEE Transactions on Pattern Analysis and Machine Intelligence*, 29(3):394–410, 2007.
- [3] X. Chen and A. Gupta. Webly supervised learning of convolutional networks. In *Proc. of IEEE International Conference on Computer Vision (ICCV)*, 2015.
- [4] T.-S. Chua, J. Tang, R. Hong, H. Li, Z. Luo, and Y. Zheng. NUS-WIDE: A real-world web image database from national university of singapore. In *Proc. of ACM International Conference on Image and Video Retrieval (CIVR)*, 2009.
- [5] M. Davis, S. King, N. Good, and R. Sarvas. From context to content: Leveraging context to infer media metadata. In *Proc. of ACM International Conference on Multimedia (ACM-MM)*, 2004.
- [6] J. Deng, W. Dong, R. Socher, L. Li, Kai Li, and Li Fei-Fei. ImageNet: A large-scale hierarchical image database. In *Proc. of IEEE Conference on Computer Vision and Pattern Recognition (CVPR)*, 2009.
- [7] S. K. Divvala, A. Farhadi, and C. Guestrin. Learning everything about anything: Webly-supervised visual concept learning. In *Proc. of IEEE Conference on Computer Vision and Pattern Recognition (CVPR)*, 2014.
- [8] K. Duan, D. Crandall, and D. Batra. Multimodal learning in loosely-organized web images. In *Proc. of IEEE Conference on Computer Vision and Pattern Recognition (CVPR)*, 2014.
- [9] N. Dvornik, J. Mairal, and C. Schmid. Modeling visual context is key to augmenting object detection datasets. In *Proc. of European Conference on Computer Vision (ECCV)*, 2018.
- [10] R. Fergus, L. Fei-Fei, P. Perona, and A. Zisserman. Learning object categories from google’s image search. In *Proc. of IEEE International Conference on Computer Vision (ICCV)*, 2005.
- [11] Y. Gong, Y. Jia, A. Toshev, T. Leung, and S. Ioffe. Deep convolutional ranking for multilabel image annotation. In *Proc. of International Conference on Learning Representations (ICLR)*, 2014.
- [12] Y. Gong, Q. Ke, M. Isard, and S. Lazebnik. A multi-view embedding space for internet images, tags, and their semantics. *International Journal of Computer Vision*, 106(2):210–233, 2014.
- [13] M. Guillaumin, T. Mensink, J. Verbeek, and C. Schmid. Tagprop: Discriminative metric learning in nearest neighbor models for image auto-annotation. In *Proc. of IEEE International Conference on Computer Vision (ICCV)*, 2009.
- [14] M. Guillaumin, J. Verbeek, and C. Schmid. Multimodal semi-supervised learning for image classification. In *Proc. of IEEE Conference on Computer Vision and Pattern Recognition (CVPR)*, 2010.
- [15] J. Hays and A. A. Efros. IM2GPS: estimating geographic information from a single image. In *Proc. of IEEE Conference on Computer Vision and Pattern Recognition (CVPR)*, 2008.
- [16] K. He, X. Zhang, S. Ren, and J. Sun. Delving deep into rectifiers: Surpassing human-level performance on imagenet classification. In *Proc. of IEEE International Conference on Computer Vision (ICCV)*, 2015.
- [17] H. Hu, G.-T. Zhou, Z. Deng, Z. Liao, and G. Mori. Learning structured inference neural networks with label relations. *Proc. of IEEE Conference on Computer Vision and Pattern Recognition (CVPR)*, 2016.
- [18] S. J. Hwang and K. Grauman. Learning the relative importance of objects from tagged images for retrieval and cross-modal search. *International Journal of Computer Vision*, 100(2):134–153, 2012.
- [19] Y. Jia, E. Shelhamer, J. Donahue, S. Karayev, J. Long, R. Girshick, S. Guadarrama, and T. Darrell. Caffe: Convolutional architecture for fast feature embedding. *arXiv preprint:1408.5093*, 2014.
- [20] J. Johnson, L. Ballan, and L. Fei-Fei. Love thy neighbors: Image annotation by exploiting image metadata. In *Proc. of IEEE International Conference on Computer Vision (ICCV)*, 2015.
- [21] A. Krizhevsky, I. Sutskever, and G. Hinton. ImageNet classification using deep convolutional neural networks. In *Proc. of Conference on Neural Information Processing Systems (NeurIPS)*, 2012.
- [22] V. Lavrenko, R. Manmatha, and J. Jeon. A model for learning the semantics of pictures. In *Proc. of Conference on Neural Information Processing Systems (NeurIPS)*, 2003.
- [23] L.-J. Li and L. Fei-Fei. OPTIMOL: Automatic online picture collection via incremental model learning. *International Journal of Computer Vision*, 88(2):147–168, 2010.
- [24] X. Li, T. Uricchio, L. Ballan, M. Bertini, C. Snoek, and A. Del Bimbo. Socializing the semantic gap: A comparative survey on image tag assignment, refinement and retrieval. *ACM Computing Surveys*, 49(1):14:1–14:39, 2016.
- [25] F. Liu, T. Xiang, T. M. Hospedales, W. Yang, and C. Sun. Semantic regularisation for recurrent image annotation. In *Proc. of IEEE Conference on Computer Vision and Pattern Recognition (CVPR)*, 2017.
- [26] C. Long, R. Collins, E. Swears, and A. Hoogs. Deep neural networks in fully connected crf for image labeling with social network metadata. In *Proc. of IEEE Winter Conference on Applications of Computer Vision (WACV)*, 2019.
- [27] A. Makadia, V. Pavlovic, and S. Kumar. A new baseline for image annotation. In *Proc. of European Conference on Computer Vision (ECCV)*, 2008.
- [28] J. McAuley and J. Leskovec. Image labeling on a network: Using social-network metadata for image classification. In *Proc. of European Conference on Computer Vision (ECCV)*, 2012.
- [29] T. Mikolov, I. Sutskever, K. Chen, G. S. Corrado, and J. Dean. Distributed representations of words and phrases and their compositionality. In *Proc. of Conference on Neural Information Processing Systems (NeurIPS)*, 2013.
- [30] Z. Niu, G. Hua, X. Gao, and Q. Tian. Semi-supervised relational topic model for weakly annotated image recognition in social media. In *Proc. of IEEE Conference on Computer Vision and Pattern Recognition (CVPR)*, 2014.

- [31] A. Oliva and A. Torralba. The role of context in object recognition. *Trends in Cognitive Sciences*, 11(12):520–527, 2007.
- [32] C. Rupprecht, A. Kapil, N. Liu, L. Ballan, and F. Tombari. Learning without prejudice: Avoiding bias in webly-supervised action recognition. *Computer Vision and Image Understanding*, 173:24–32, 2018.
- [33] C. Saedi, A. Branco, J. António Rodrigues, and J. Silva. WordNet embeddings. In *Proc. of ACL Workshop on Representation Learning for NLP*, 2018.
- [34] K. Tang, M. Paluri, L. Fei-Fei, R. Fergus, and L. Bourdev. Improving image classification with location context. In *Proc. of IEEE International Conference on Computer Vision (ICCV)*, 2015.
- [35] A. Torralba. Contextual priming for object detection. *International Journal of Computer Vision*, 53(2):169–191, 2003.
- [36] T. Uricchio, L. Ballan, L. Seidenari, and A. Del Bimbo. Automatic image annotation via label transfer in the semantic space. *Pattern Recognition*, 71:144–157, 2017.
- [37] Y. Verma and C. Jawahar. Image annotation using metric learning in semantic neighbourhoods. In *Proc. of European Conference on Computer Vision (ECCV)*, 2012.
- [38] G. Wang, D. Hoiem, and D. Forsyth. Learning image similarity from flickr groups using fast kernel machines. *IEEE Transactions on Pattern Analysis and Machine Intelligence*, 34(11):2177–2188, 2012.
- [39] J. Wang, Y. Yang, J. Mao, Z. Huang, C. Huang, and W. Xu. CNN-RNN: A unified framework for multi-label image classification. In *Proc. of IEEE Conference on Computer Vision and Pattern Recognition (CVPR)*, 2016.
- [40] A. Yu and K. Grauman. Predicting useful neighborhoods for lazy local learning. In *Proc. of Conference on Neural Information Processing Systems (NeurIPS)*, 2014.
- [41] A. Zamir, S. Ardesir, and M. Shah. Gps-tag refinement using random walks with an adaptive damping factor. In *Proc. of IEEE Conference on Computer Vision and Pattern Recognition (CVPR)*, 2014.
- [42] J. Zhang, Q. Wu, J. Zhang, C. Shen, and J. Lu. Mind your neighbours: Image annotation with metadata neighbourhood graph co-attention networks. In *Proc. of IEEE Conference on Computer Vision and Pattern Recognition (CVPR)*, 2019.
- [43] F. Zhu, H. Li, W. Ouyang, N. Yu, and X. Wang. Learning spatial regularization with image-level supervisions for multi-label image classification. In *Proc. of IEEE Conference on Computer Vision and Pattern Recognition (CVPR)*, 2017.